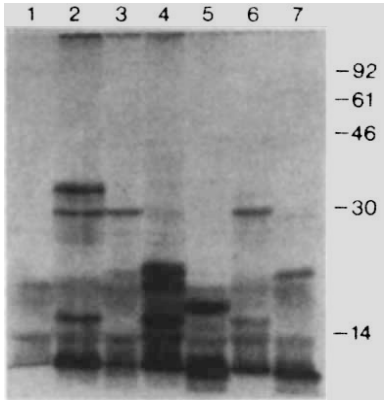

Fig. 4 *In vitro* translation of NGF RNA. For the longer construction containing both potential initiator AUGs (at +98 and +296 in the nucleotide sequence of the NGF mRNA), the cDNA was digested with *Sma*I (+66) and *Pst*I (+1027) and inserted into the SP65 vector. For the shorter construction containing only the second potential initiation codon, the cDNA was partially digested with *Bst*XI (+184), then *Pst*I and inserted into the same vector. Following linearization with the enzymes designated below, the two constructions (named LmRNA and SmRNA for the longer and shorter, respectively) were then used as templates for RNA synthesis with the SP6 polymerase[38]. This RNA was then translated *in vitro* by the wheat germ system in the presence of ^{35}S-methionine[39]. The protein products were precipitated in 10% trichloracetic acid and subjected to electrophoresis on 12% SDS-polyacrylamide. The gel was enhanced with I M sodium salicylate and exposed overnight at −70 °C with an enhancing screen, Lane 1, no RNA; lane 2, LmRNA linearized with *Hin*dIII (3′ to the inserted cDNA); lane 3, SmRNA linearized with *Hin*dIII; lane 4, LmRNA linearized with *Nco*I (at +616 in the cDNA); lane 5, SmRNA linearized with *Nco*I; lane 6, LmRNA linearized with *Sca*I (at +810 in the cDNA); lane 7, SmRNA linearized with *Sca*I; numbers on the right indicate the M_rs of the protein standards ($\times 10^3$).

do not prove alternative use of the two AUGs *in vivo*, they do show that the translational apparatus can recognize both AUGs.

An understanding of the biological significance of differential splicing in the expression of NGF requires further information about the functions of the various precursor molecules. The NGF precursor contains several di- and tetrabasic residues that are potential peptidase cleavage sites (Fig. 3*c*). The small NGF precursor protein derived from the shorter transcript retains these sites, but the potential NH_2-terminal cleavage product would be truncated. If the full precursor or one of its derived peptides has biological activity, the two RNA splicing pathways could result in differing biological effects. It is intriguing that the two transcripts result in proteins with the hydrophobic sequence in different positions; in the long precursor, it resides in the middle of the molecule and might serve as a membrane anchor (similar to the epidermal growth factor precursor in the kidney[24]); in the short precursor, the hydrophobic region is at the N-terminus, and may act as a signal peptide to ensure secretion[25]. Differential splicing could therefore affect cellular localization, as with IgM and yeast invertase[26,27]. Although the short transcript presumably results in a secreted NGF that can act at a distance, the long transcript might produce a form of NGF that is membrane-bound and could interact with high efficiency at a receptor on a contiguous cell; these mechanisms could provide the basis for direct cell-cell communication.

We thank Dr David Standring for advice on the RNA analysis, Drs Jang Han and Jeff Edman for help with cDNA synthesis, Drs James Ou, Michael Walker and Eric Fodor for their thoughtful discussion, Drs Pablo Garcia and Peter Walter for assistance with *in vitro* translation, Dr Philip Barr for the oligonucleotides, and Ms Leslie Spector for preparing the manuscript. R.H.E. was supported by a postdoctoral fellowship from the NINCDS (NS07529-02). This research was supported by NIH grant AM 21334 (to W.J.R.).

Received 20 August 1985; accepted 2 January 1986.

1. Levi-Montalcini, R. & Angeletti, P. U. *Pharmac. Rev.* **18,** 619-628 (1966).
2. Gorin, P. D. & Johnson, E. M. *Proc. natn. Acad. Sci. U.S.A.* **76,** 5382-5386 (1979).
3. Stockel, K., Schwab, M. E. & Thoenen, H. *Brain Res.* **99,** 1-16 (1975).
4. Banks, B. E. C. *et al. J. Physiol., Lond.* **247,** 289-298 (1975).
5. Chun, L. L. Y. & Patterson, P. H. *J. Cell Biol.* **75,** 694-704 (1975).
6. Thoenen, H. & Barde, Y-A. *Physiol. Rev.* **60,** 1284-1335 (1980).
7. Mobley, W. C. *et al. Science* **229,** 284-287 (1985).
8. Ullrich, A. *et al. Nature* **303,** 821-825 (1983).
9. Murphy, R. A. *et al. Proc. natn. Acad. Sci. U.S.A.* **74,** 4496-4500 (1977).
10. Oger, J. O. *et al. Proc. natn. Acad. Sci. U.S.A.* **71,** 1554-1558 (1974).
11. Scott, J. *et al. Nature* **302,** 538-540 (1983).
12. Shelton, D. L. & Reichardt, L. F. *Proc. natn. Acad. Sci. U.S.A.* **81,** 7951-7955 (1984).
13. Harper, G. P. *et al. Nature* **279,** 160-162 (1979).
14. Herbert, E. *et al. Cold Spring Harb. Symp. quant. Biol.* **47,** 375-384 (1983).
15. Amara, S. G. *et al. Nature* **298,** 240-244 (1982).
16. Nawa, H., Kotani, H. & Nakanishi, S. *Nature* **312,** 729-734 (1984).
17. Falkenthal, S., Parker, V. P. & Davidson, N. *Proc. natn. Acad. Sci. U.S.A.* **82,** 449-453 (1985).
18. Medford, R. M. *et al. Cell* **38,** 409-421 (1984).
19. Mount, S. *Nucleic Acids Res.* **10,** 459-472 (1982).
20. Steitz, J. A. *et al. Cold Spring Harb. Symp. quant. Biol.* **47,** 893-900 (1983).
21. Mount, S. M. *et al. Cell* **33,** 509-518 (1983).
22. Kozak, M. *Nucleic Acids Res.* **9,** 5233-5252 (1981).
23. Darling, T. L. J. *et al. Cold Spring Harb. Symp. quant. Biol.* **48,** 427-534 (1983).
24. Rall, L. *et al. Nature* **313,** 228-233 (1985).
25. Lingappa, V. R. *et al. Proc. natn. Acad. Sci. U.S.A.* **75,** 2338-2342 (1978).
26. Early, P. *et al. Cell* **20,** 313-319 (1980).
27. Carlson, M. & Botstein, D. *Cell* **28,** 145-154 (1982).
28. Chirgwin, J. M. *et al. Biochemistry* **18,** 5294-52?? (1979).
29. Cathala, G. *et al. DNA* **2,** 329-335 (1983).
30. Aviv, H. & Leder, P. *Proc. natn. Acad. Sci. U.S.A.* **69,** 1408-1412 (1972).
31. Berk, A. J. & Sharp, P. A. *Cell* **12,** 721-732 (1977).
32. Hu, N. T. & Messing, J. *Gene* **17,** 271-277 (1982).
33. McKnight, S. L. & Kingsbury, R. *Science* **217,** 316-324 (1982).
34. Wallace, R. B. *et al. Nucleic Acids Res.* **9,** 2647-2656 (1981).
35. Okayama, H. & Berg, P. *Molec. cell. Biol.* **2,** 161-170 (1982).
36. Huynh, T. V., Young, R. A. & Davis, R. W. in *DNA Cloning Techniques: A Practical Approach* (ed. Glover, D.) pp. 49-78 (IRL Press, Oxford, 1984).
37. Sanger, F., Nicklen, S. & Coulson, A. R. *Proc. natn. Acad. Sci. U.S.A.* **74,** 5463-5467 (1977).
38. Krieg, P. A. & Melton, D. A. *Nucleic Acids Res.* **12,** 7057-7070 (1984).
39. Erickson, A. H. & Blobel, G. *Meth. Enzym.* **96,** 38-50 (1983).

Cell contact- and shape-dependent regulation of vinculin synthesis in cultured fibroblasts

Florette Ungar*, Benjamin Geiger† & Avri Ben-Ze'ev*

Departments of *Genetics and †Chemical Immunology, Weizmann Institute of Science, Rehovot, Israel 76100

Recent studies have demonstrated the fundamental role of cell-substrate contacts and changes in cell shape in the regulation of cell growth, motility and differentiation[1–7], but the molecular basis for these phenomena is poorly understood. Because of the involvement of cytoskeletal networks in cell morphogenesis and contact formation, it is of interest that the expression of genes encoding several cytoskeletal proteins is markedly affected by changes in cell contacts and configuration[6–10]. Because most of these phenomena involve changes in the form, extent or topology of cell contacts, we sought to determine whether the expression of components directly involved in the formation of cell–cell or cell–substrate contacts is affected by the respective cellular interactions. A suitable candidate for such analysis is vinculin, a cytoskeletal protein of relative molecular mass (M_r) 130,000 (130K), which is localized in focal contacts[11–13] and intercellular adherens junctions[14]. The assembly of vinculin into a membrane-bound junctional plaque seems to be one of the earliest cellular responses to contact with exogenous substrates, leading to the subsequent local assembly of the actin-rich microfilament bundles[15,16]. Here we report on the regulation of vinculin synthesis in response to environmental conditions that affect cell shape and contacts.

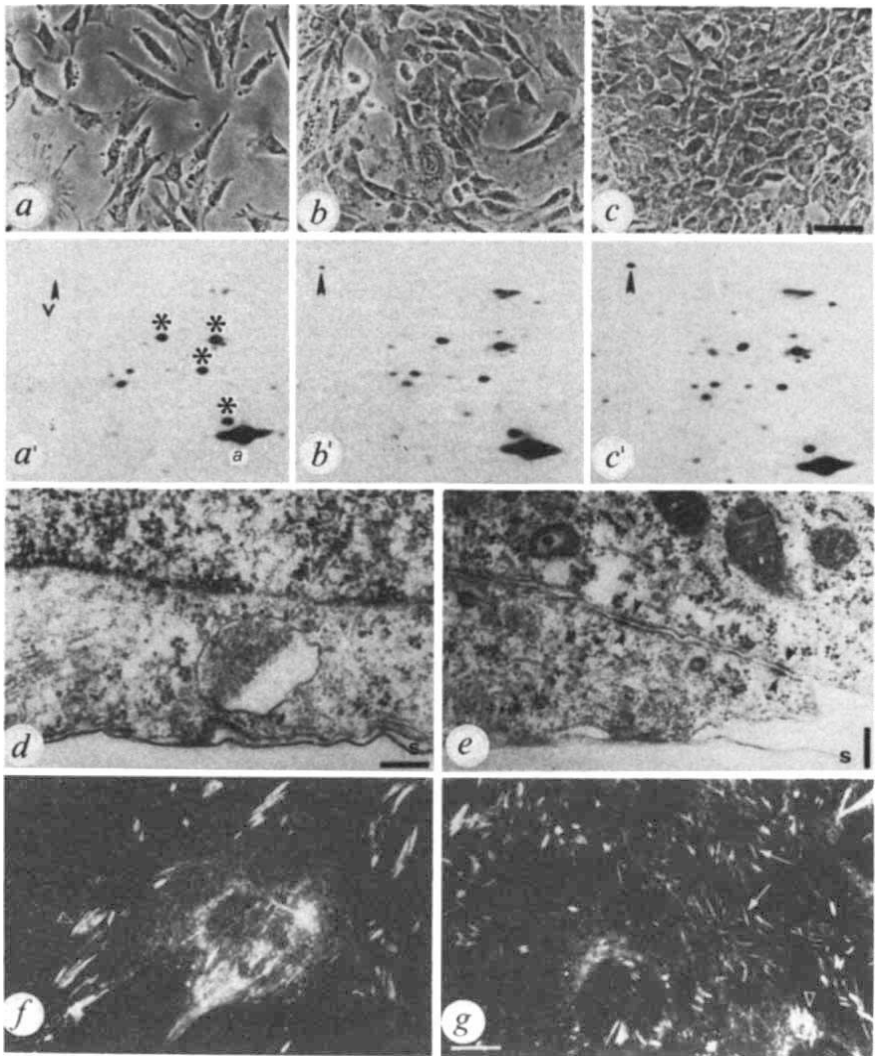

Fig. 1 Vinculin synthesis and cell-contact formation in 3T3 cells plated at different densities. *a–c*, Phase-contrast photomicrographs of Swiss 3T3 fibroblasts plated for 2 days at concentrations of 2×10^4 (*a*), 10^5 (*b*) and 5×10^5 (*c*) cells per 35-mm Falcon tissue-culture dish. *a′–c′*, Analysis of proteins from corresponding samples labelled for 4 h with 100 μCi ml^{-1} ^{35}S-methionine. Extracts were prepared by scraping cells into a buffer containing 1.0% Triton X-100, 0.6 M KCl, 5 mM EGTA, 7 mM 2-mercaptoethanol, 1 mM phenylmethylsulphonyl fluoride and 10 mM Tris-HCl (*p*H 7.4) and combining the supernatant with that obtained after treatment of the pellet with DNase I and then with 0.6 M KCl. Equal amounts of TCA-insoluble radioactivity (5×10^5 c.p.m. per sample) were analysed by two-dimensional gel electrophoresis as described previously[25]. *a*, Actin; v and arrowheads point to vinculin. Asterisks mark proteins whose intensity of labelling did not change and which served as reference spots. *d*, *e*, Electron micrographs of 3T3 cells plated at a density of either 2×10^4 cells per dish (*d*) or 5×10^5 cells per dish (*e*) for 2 days. Cells were fixed in the dish with 1% glutaraldehyde in 0.1 M cacodylate buffer *p*H 7.2, postfixed in 1% OsO_4, flat-embedded in Epon and sectioned perpendicular to the plane of the dish. s, Substrate; arrowheads point to intercellular adherens-type junctions with submembrane electron density. *f*, *g*, Indirect immunofluoresence staining of sparse (*f*) and dense (*g*) 3T3 cultures with a monoclonal antibody against chicken gizzard vinculin and rhodaminated goat anti-mouse IgG. Arrowheads point to large vinculin-containing adhesion plaques; arrows mark thin vinculin-containing structures corresponding to cell–cell contacts. Scale bars: *a–c*, 50 μm; *d*, *e*, 0.2 μm; *f*, *g*, 10 μm.

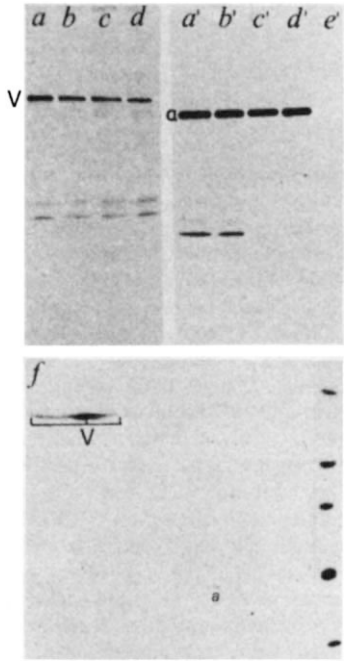

Fig. 2 Identification of vinculin in sparse and dense cultures of 3T3 cells by immunoprecipitation with a monoclonal, vinculin-specific antibody. 3T3 cultures on 35-mm dishes which had been seeded with either 5×10^5 cells (*a*, *a′*, *e′*), 2.5×10^5 cells (*b*, *b′*), 10^5 cells (*c*, *c′*) or 2×10^4 cells (*d*, *d′*) were labelled for 4 h with ^{35}S-methionine and lysed in RIPA buffer (10 mM NaH_2PO_4, 100 mM NaCl, 1.0% Triton X-100, 0.5% sodium deoxycholate, 0.1% SDS, *p*H 7.0). We took 2×10^6 c.p.m. from each culture for immunoprecipitation with either anti-vinculin antibody (*a–d*, *f*), anti-α-actinin antibody (*a′–d′*) or non-immune mouse immunoglobulin (*e′*). The immune complexes were precipitated by binding to *Staphylococcus aureus*, according to Kessler[26]. *a–d*, *a′–e′*, Analysis on 10% acrylamide gels; *f*, two-dimensional gel analysis of immunoprecipitate from 5×10^5 cells labelled as above. α, α-Actinin; V, vinculin (all isoforms); a, actin. Relative molecular mass markers for the gel include (top to bottom) myosin heavy chains, phosphorylase *b*, bovine serum albumin, ovalbumin and carbonic anhydrase.

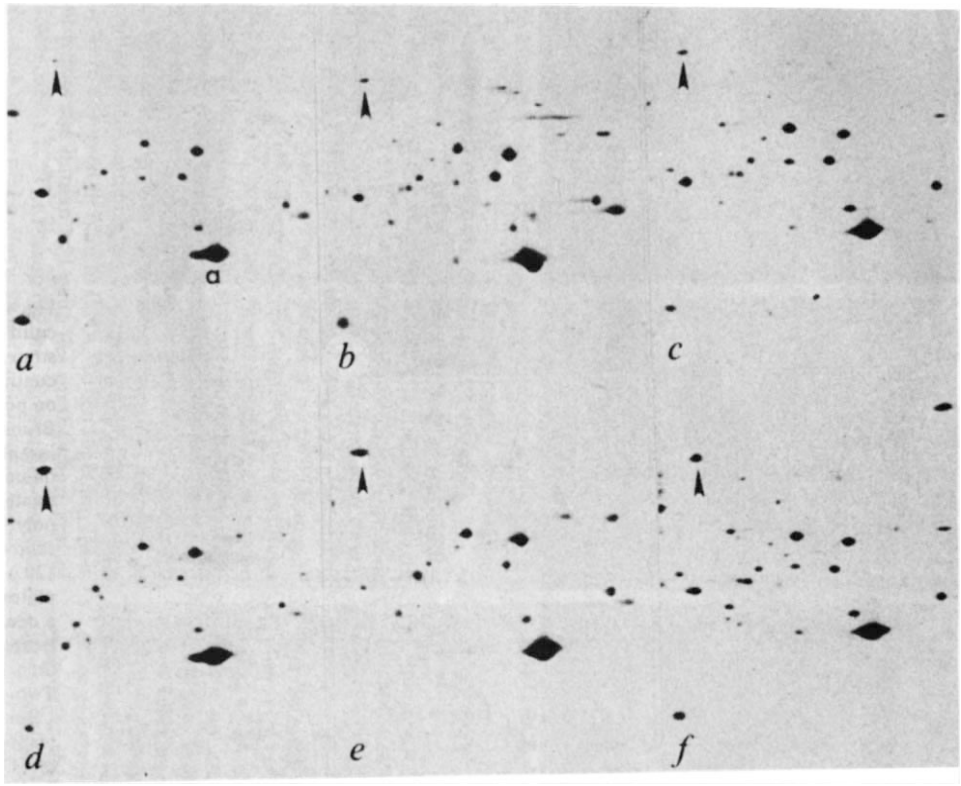

Fig. 3 Vinculin synthesis in sparse and dense 3T3 cultures determined by ^{35}S-methionine pulses and by pulse-chase experiments. 3T3 cells plated at 2×10^4 cells per 35-mm dish (*a–c*) or at 5×10^5 cells per 35-mm dish (*d–f*) were either labelled for 45 min with 400 μCi ml^{-1} of ^{35}S-methionine (*a, d*) or labelled for 45 min as above and then washed extensively and further incubated in medium containing unlabelled methionine for 10 h (*b, e*). Alternatively, cells were continuously labelled for 11 h with 40 μCi ml^{-1} of ^{35}S-methionine (*c, f*). Cell extracts containing 5×10^5 c.p.m. from each sample were analysed by two-dimensional gel electrophoresis as in Fig. 1. Arrowheads point to vinculin; reference spots were as in Fig. 1; a, actin.

To examine the role of specific cell contacts in the regulation of vinculin expression, we plated primary chicken fibroblasts or Swiss 3T3 cells at increasing densities on tissue-culture dishes. At a low plating density, cells were spread out on the substrate, rarely contacting each other. At higher densities, cell–cell contacts became prominent, the extent of spreading was limited and most cells assumed an elongated, cylindrical shape (Fig. 1 *a–c*). To compare the rate of vinculin synthesis by the different cultures, cells were labelled with ^{35}S-methionine, equal trichloroacetic acid (TCA)-precipitable labelled polypeptides were resolved by two-dimensional gel electrophoresis and the radioactivity associated with the vinculin spots was measured and normalized against several standard polypeptides on the same gels (Fig. 1*a′–c′*). Vinculin labelling was enhanced sevenfold when cell density was increased (Table 1).

Electron microscope examination of sparse and dense cultures of 3T3 cells revealed that the ventral membrane of sparse cells (Fig. 1*d*) was usually closer to the substrate than that of cells in dense cultures (Fig. 1*e*) (mean distance from the substrate = 25 nm, compared with ~60 nm in the latter). In dense cultures, however, many focal contacts were detected, as well as areas of tight cell–cell contact (arrowheads in Fig. 1*e*). Immunofluorescence staining with anti-vinculin antibody revealed that the protein was associated mainly with large ventral focal contacts in sparse cultures of 3T3 cells, and in dense monolayer cultures vinculin staining was observed both in small focal contacts and in many cell–cell contacts located above the plane of the substrate (Fig. 1*g*, arrows), in agreement with the electron microscope observations. To substantiate the suggestion that cell density affects vinculin synthesis, cell extracts of ^{35}S-methionine-labelled cultures at different densities were subjected to two-dimensional gel analysis or to immunoprecipitation with either anti-vinculin or anti-α-actinin (used as a control). The results confirmed that the 130K protein, whose labelling was augmented by the increase in cell density, was immunochemically (Fig. 2*a–d*) and biochemically (Fig. 2*f*) identical to vinculin. In chicken fibroblasts, which displayed an essentially identical increase in vinculin expression (Table 1), we also examined the iodinated peptide map of the 130K spot and found it to be identical to that of purified chicken gizzard vinculin (data not shown).

To determine whether the changes in incorporation of ^{35}S-methionine into vinculin are caused by altered rates of synthesis or of turnover, we labelled sparse and dense 3T3 cultures for various periods of time and also carried out pulse-chase experiments (Fig. 3). Densitometric examination of the vinculin spots in comparison with control proteins (see Fig. 1) indicated that the ratio between vinculin labelling in the dense and sparse

Table 1 Relative rates of vinculin synthesis as a function of cell density and cell spreading

Cell type	Plating density per 35 mm dish	Relative rate of vinculin synthesis	Poly(HEMA) concentration (μg ml^{-1})	Relative rate of vinculin synthesis
3T3	2.0×10^4	1.0	None	1.0
	2.0×10^5	3.75	72	0.53
	3.0×10^5	4.5	96	0.63
	5.0×10^5	7.0	120	0.28
			1,200	0.21
Chicken gizzard	2.5×10^4	1.0	ND	ND
	10^5	2.7	ND	ND
	2.5×10^5	5.3	ND	ND
	10^6	6.8	ND	ND

Cells were plated on 35-mm diameter dishes and after 2 days were labelled with ^{35}S-methionine as described in Fig. 1 legend. The intensity of the vinculin spot on two-dimensional gels was determined by densitometric scanning and normalized against several reference spots whose intensity did not change (asterisks, Fig. 1). 3T3 cells were also seeded on poly(HEMA)-coated plates as outlined in Fig. 4, labelled with ^{35}S-methionine and analysed on two-dimensional gels. ND, not done.

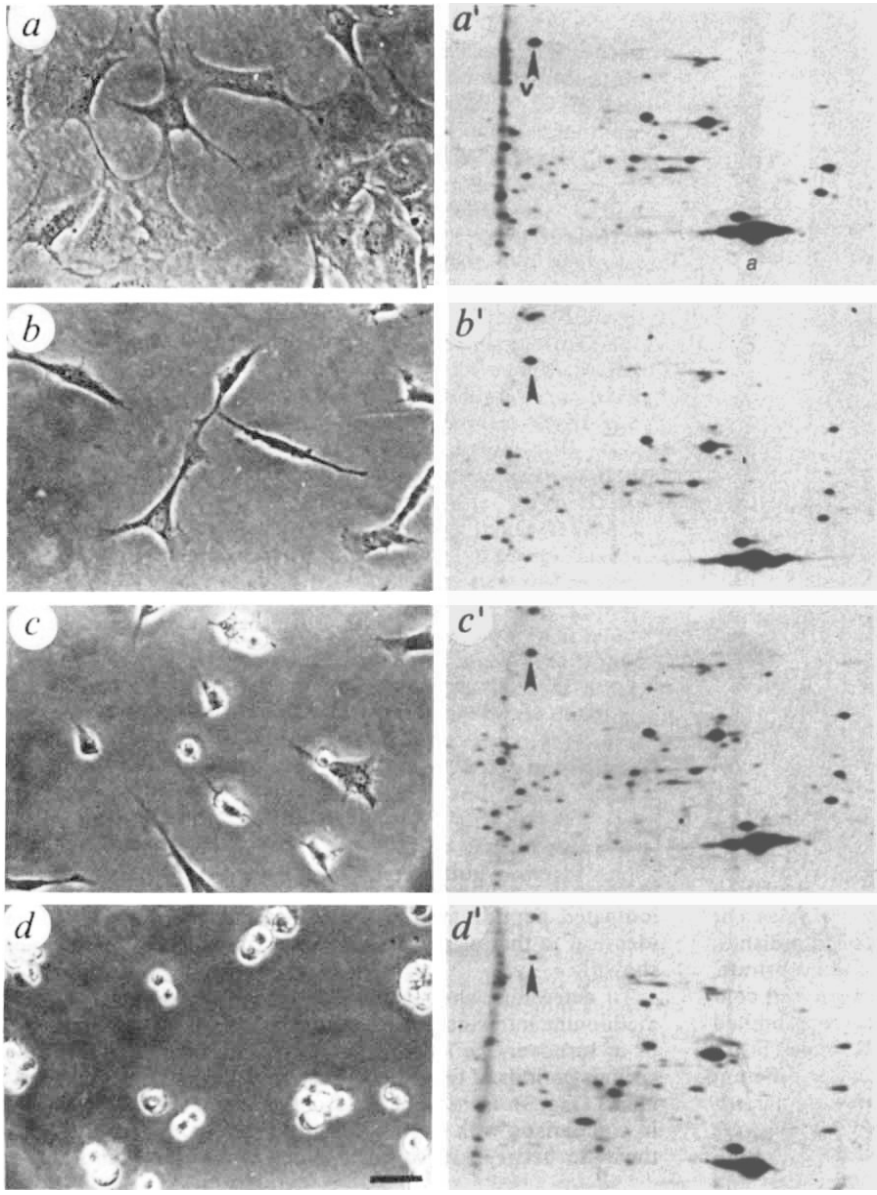

Fig. 4 Analysis of cell morphology and vinculin synthesis in 3T3 cells plated on substrates of varying adhesiveness. *a–d*, Phase-contrast photomicrographs of 3T3 cells grown on poly(HEMA) (Hydron Laboratories, New Brunswick) coated plastic plates prepared essentially as described elsewhere[2,3]. Plastic tissue-culture plates (5 cm diameter) were treated with 2.5 ml of either ethanol (*a*) or poly(HEMA)–ethanolic solutions of the following concentrations: 96 $\mu g\,ml^{-1}$ (*b*); 120 $\mu g\,ml^{-1}$ (*c*); or 1,200 $\mu g\,ml^{-1}$ (*d*). The plates were dried at 37 °C for 2 days. Cells at a density of 10^5 per plate were seeded on the treated substrates and incubated for 2 days, then labelled as described for Fig. 1. *a'–d'*, Two-dimensional gel electrophoresis of the ^{35}S-methionine-labelled proteins from the respective samples, containing equal amounts of TCA-insoluble radioactivity. Cell labelling and cell extracts were prepared as described in Fig. 1. Arrowheads point to vinculin; a, actin; reference proteins, whose intensity of labelling did not change, are as in Fig. 1.

cultures was not significantly affected by the duration of the labelling period (Fig. 3*a*, *b*, *d*, *e*) or in pulse-chase experiments (Fig. 3*c*, *f*). We therefore conclude that the extent of cell–cell interactions affects the synthesis rather than the turnover of vinculin.

To determine whether the rate of vinculin synthesis is affected by changing the extent of cell–substrate contact, we plated equal numbers of 3T3 cells on substrates of decreasing degrees of adhesiveness, using dishes coated with different concentrations of poly(2-hydroxyethyl methacrylate) (poly(HEMA; Fig. 4*a–d*; also refs 2, 3). Two days after plating, cell shape varied from well-spread on thin poly(HEMA) films (Fig. 4*a*) to spherical on dense poly(HEMA) films (Fig. 4*d*). The level of vinculin synthesis per constant amount of total ^{35}S-labelled protein was approximately fivefold lower in spherical, non-adherent cells (Fig. 4*d'*) than in flat monolayer cells (Fig. 4*a'*), with intermediate values in cells showing intermediate degrees of spreading (Fig. 4*b'*, *c'*; Table 1). Control experiments similar to those of Fig. 3 verified that vinculin synthesis rather than its turnover, was affected, suggesting that vinculin synthesis correlates with the degree of cell spreading induced by alterations of substrate adhesiveness.

The experiments described here indicate that cells express vinculin in relation to its pattern of organization in the cell and/or to the mode of cell contacts formed. The organization of vinculin is altered in dense cultures, and the protein is extensively associated with areas of cell–cell contact of the adherens type. Thus, vinculin synthesis, like that of several other cytoskeletal proteins (vimentin, actin, tubulin and cytokeratin[8–11]), is sensitive to the degree of cell–cell and/or cell–substrate contact (see refs 6, 17 for reviews). We suggest that, as well as its unique regulation by intercellular contacts, vinculin has, in common with the cytoskeletal proteins mentioned above, a feedback control mechanism for its synthesis, which can be regulated by alterations in the adhesive properties of the substrate. The level of vinculin expression cannot simply be correlated with cellular properties such as the rate of cell growth. Vinculin synthesis was lowest in sparse cell cultures, which exhibit maximal rates of cell proliferation, whereas the synthesis was maximally stimulated in the almost arrested dense

cultures (Figs 1-3). On the other hand, vinculin synthesis was found to be lowest in the spherical non-proliferating cells in experiments where the substrate was altered (Fig. 4)[1,2,9,18,19].

The association of vinculin with areas of cell-substrate contact and its rapid reorganization on addition of purified growth factors to cells arrested in the G_1 phase of the cell cycle[20], suggests that the protein is involved in the transmission of contact-dependent, growth-related signals from the exterior. Transformation of cells by Rous sarcoma virus and other oncogenic viruses induces marked alterations in vinculin and actin organization, concomitant with overall changes in cell shape and adhesiveness[21-23], phenomena also observed on addition of tumour promoters to cells[24]. These observations highlight the role of cell contacts in the regulation of cell growth and suggest that proteins such as vinculin, which are involved in the construction of these cellular structures, participate in this regulation.

This work was supported in part by a grant from the Israel-USA Binational Foundation (A.B.-Z.) and by a grant from the Erna Rothstein Foundation (B.G.).

Received 31 October 1985; accepted 2 January 1986.

1. Benecke, B. J., Ben-Ze'ev, A. & Penman, S. *Cell* **14**, 931-939 (1978).
2. Ben-Ze'ev, A., Farmer, S. R. & Penman, S. *Cell* **21**, 365-372 (1980).
3. Folkman, J. & Moscona, A. *Nature* **273**, 345-349 (1978).
4. Wittelsberger, S. C., Kleene, K. & Penman, S. *Cell* **24**, 859-866 (1981).
5. Farmer, S. R., Ben-Ze'ev, A., Benecke, B. J. & Penman, S. *Cell* **15**, 627-637 (1978).
6. Ben-Ze'ev, A. in *Cell and Muscle Motility* Vol. 6 (ed. Shay, J. W.) 23-53 (Plenum, New York, 1985).
7. Bissel, M. J., Hall, H. G. & Parry, G. *J. theor. Biol.* **99**, 31-68 (1982).
8. Ben-Ze'ev, A., Farmer, S. R. & Penman, S. *Cell* **17**, 319-325 (1979).
9. Farmer, S. R. Wan, K. M., Ben-Ze'ev, A. & Penman, S. *Molec. cell. Biol.* **3**, 182-189 (1983).
10. Ben-Ze'ev, A. *J. Cell Biol.* **97**, 858-865 (1983); **99**, 1424-1433 (1984).
11. Geiger, B. *Cell* **18**, 193-205 (1979).
12. Burridge, K. & Fermaisco, J. *Cell* **19**, 587-595 (1980).
13. Geiger, B., Tokuyasu, K. T., Dutton, A. H. & Singer, S. J. *Proc. natn. Acad. Sci. U.S.A.* **77**, 4127-4131 (1980).
14. Geiger, B., Dutton, A. H., Tokuyasu, K. T. & Singer, S. J. *J. Cell Biol.* **91**, 614-628 (1981).
15. Geiger, B. *Cold Spring Harb. Symp. quant. Biol.* **46**, 671-682 (1982).
16. Geiger, B., Avnur, Z., Kreis, T. E. & Schlessinger, J. in *Cell and Muscle Motility* Vol. 5 (ed. Shay, J. W.) 195-234 (Plenum, New York, 1984).
17. Ben-Ze'ev, A. in *Molecular Biology of the Cytoskeleton* (eds Borisy, G., Cleveland, D. & Murphy, D.) 435-444 (Cold Spring Harbor Laboratory, New York, 1985).
18. Johnson, L. F., Abelson, H. T., Green, H. & Penman, S. *Cell* **1**, 95-100 (1974).
19. Otsuka, H. & Moskowitz, M. *J. cell. Physiol.* **89**, 213-220 (1976).
20. Herman, B. & Pledger, W. J. *J. Cell Biol.* **100**, 1031-1040 (1985).
21. David-Pfeuty, T. & Singer, S. J. *Proc. natn. Acad. Sci. U.S.A.* **77**, 6687-6691 (1980).
22. Sefton, B. M., Hunter, T., Ball, E. H. & Singer, S. J. *Cell* **24**, 165-174 (1981).
23. Shriver, K. & Rohrschneider, L. *J. Cell Biol.* **89**, 525-535 (1981).
24. Schliwa, M., Nakamura, T., Porter, K. R. & Euteneuer, U. *J. Cell Biol.* **99**, 1045-1059 (1984).
25. O'Farrell, P. H. *J. biol. Chem.* **250**, 4007-4021 (1975).
26. Kessler, S. W. *J. Immun.* **115**, 1617-1624 (1975).

Stable transformation of maize after gene transfer by electroporation

Michael E. Fromm, Loverine P. Taylor & Virginia Walbot

Department of Biological Sciences, Stanford University, Stanford, California 94305-2493, USA

The graminaceous monocots, including the economically important cereals, seem to be refractory to infection by *Agrobacterium tumefaciens*[1], a natural gene transfer system that has been successfully exploited for transferring foreign genes into higher plants[2-4]. Therefore, direct transfer techniques that are potentially applicable to all plant species have been developed using a few dicot[5-8] and monocot[8-10] species as model systems. One of these techniques, electroporation, uses electrical pulses of high field strength to permeabilize cell membranes[11] reversibly so as to facilitate the transfer of DNA into cells[8,12,13]. Electroporation-mediated gene transfer has resulted in stably transformed animal cells[12,13] and transient gene expression in monocot and dicot plant cells[8]. Here we report that electroporation-mediated DNA transfer of a chimaeric gene encoding neomycin phosphotransferase results in stably transformed maize cells that are resistant to kanamycin.

The neomycin phosphotransferase II (*npt-II*) gene from the transposon Tn*5* (ref. 14) is a useful dominant marker in both animal[15] and plant[3,16,17] cells when expressed using the appropriate eukaryotic regulatory signals. Expression of the *npt-II* coding region confers resistance to the antibiotics kanamycin and G418, to which plant cells are normally sensitive[3,16,17]. We demonstrated previously that the cauliflower mosaic virus (CaMV) 35S promoter (nucleotides 7,017-7,437, see ref. 18 for nucleotide numbers) and the nopaline synthase 3′ region[19] were sufficient 5′ and 3′ regulatory signals to express the chloramphenicol acetyltransferase coding region in maize protoplasts[8]. Accordingly, the CaMV 35S promoter, the *npt-II* coding region and the nopaline synthase 3′ region were used to construct pCaMVNEO (Fig. 1) to serve as a selectable marker in maize. pCaMVNEO expresses detectable *npt-II* enzyme activity 20 h after electroporation-mediated transfer into maize protoplasts (data not shown), demonstrating that it can be expressed in maize cells and therefore should confer resistance to kanamycin in transformed cells.

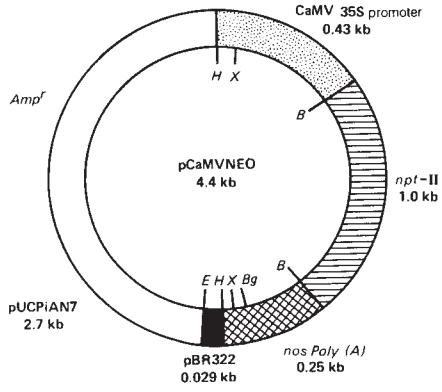

Fig. 1 Diagram of pCaMVNEO. The size in kilobase pairs is shown next to each DNA fragment composing pCaMVNEO, with the source of each fragment represented by a different background: stippled, cauliflower mosaic virus 35S promoter; hatched, neomycin phosphotransferase II; cross-hatched, nopaline synthase (*nos*) polyadenylation region; black, pBR322; white, pUCPiAN7. Relevant restriction sites are also indicated: B, *Bam*HI; Bg, *Bgl*II; E, *Eco*RI; H, *Hin*dIII; X, *Xba*I.

Methods. pUCPiAN7 contains the polylinker of PiAN7 (Biolabs) inserted into PUC8[31]. A 777-base pair (bp) *Hin*cII fragment (nucleotides 7,017-7,794, see ref. 18 for nucleotide numbers) from CaMV strain 1841 (ref. 32) containing the CaMV 35S promoter was inserted into the *Hin*cII site of pUC8. A 430-bp fragment (nucleotides 7,017-7,437) was excised with *Eco*RI and *Hph*I, then inserted into *Eco*RI, *Hin*cII cleaved pUC8. This 430-bp CaMV 35S promoter fragment was then excised as a *Bam*HI-*Pst*I fragment and inserted into pUCPiAN7, which had been double digested with *Bgl*II and *Pst*I to yield pCaMV. The 250-bp *Sau*3A fragment spanning the polyadenylation region of the *nos* gene[3] was sequentially inserted into the *Bgl*II site of pUCPiAN7, then into pBR322 as a *Hin*dIII-*Bam*HI fragment, followed by insertion into pCaMV as an *Eco*RI-*Bam*HI fragment. This yields the plasmid pCaMVNOS that contains a unique *Bam*HI site between the CaMV 35S promoter and the *nos* polyadenylation region. A 1.0-kb *Bam*HI fragment of the *npt-II* gene spanning nucleotides 1,540-2,518[14] was inserted into the *Bam*HI site of pCaMVNOS to yield pCaMVNEO. The nucleotide position corresponding to the 5′ end of the CaMV 35S RNA[18] (nucleotide 7,435) is located 17 bp upstream of the *Bam*HI site at the 5′ end of the *npt-II* gene fragment shown.